

University of New Hampshire
University of New Hampshire Scholars' Repository

Master's Theses and Capstones

Student Scholarship

Fall 2007

Kaon nucleon scattering in lattice QCD

Anthony Charles Marcolongo
University of New Hampshire, Durham

Follow this and additional works at: <https://scholars.unh.edu/thesis>

Recommended Citation

Marcolongo, Anthony Charles, "Kaon nucleon scattering in lattice QCD" (2007). *Master's Theses and Capstones*. 305.
<https://scholars.unh.edu/thesis/305>

This Thesis is brought to you for free and open access by the Student Scholarship at University of New Hampshire Scholars' Repository. It has been accepted for inclusion in Master's Theses and Capstones by an authorized administrator of University of New Hampshire Scholars' Repository. For more information, please contact nicole.hentz@unh.edu.

KAON NUCLEON SCATTERING IN LATTICE QCD

BY

ANTHONY CHARLES MARCOLONGO

THESIS

Submitted to the University of New Hampshire
in partial fulfillment of
the requirements for the degree of

Master of Science

in

Physics

September 2007

UMI Number: 1447896

INFORMATION TO USERS

The quality of this reproduction is dependent upon the quality of the copy submitted. Broken or indistinct print, colored or poor quality illustrations and photographs, print bleed-through, substandard margins, and improper alignment can adversely affect reproduction.

In the unlikely event that the author did not send a complete manuscript and there are missing pages, these will be noted. Also, if unauthorized copyright material had to be removed, a note will indicate the deletion.

UMI[®]

UMI Microform 1447896

Copyright 2007 by ProQuest Information and Learning Company.

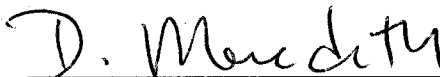
All rights reserved. This microform edition is protected against unauthorized copying under Title 17, United States Code.

ProQuest Information and Learning Company
300 North Zeeb Road
P.O. Box 1346
Ann Arbor, MI 48106-1346

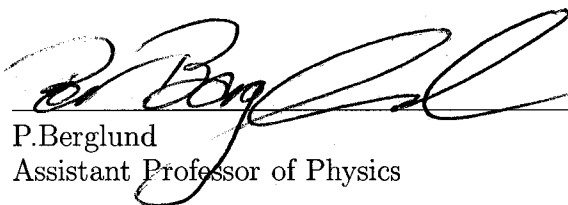
This thesis has been examined and approved.



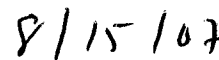
Thesis Director, S. Beane
Assistant Professor of Physics



D. Meredith
Associate Professor of Physics



P. Berglund
Assistant Professor of Physics



Date

TABLE OF CONTENTS

LIST OF TABLES	v
LIST OF FIGURES	vi
ABSTRACT	vii
1 BACKGROUND	1
1.1 General QCD	1
1.2 Mesons and Baryons	4
1.3 The Path Integral Formulation of Quantum Mechanics	5
1.3.1 Slicing the Time Dimension	6
1.3.2 The Path Integral and the Partition Function	7
1.3.3 Wick Rotation	7
1.4 Lattice QCD	8
1.4.1 Discretizing the Action	9
1.4.2 Chiral Symmetry	10
1.4.3 Chiral Perturbation Theory	12
2 DETAILS OF THE LATTICE CALCULATION	14
2.1 Details of the Lattice Calculation	14
3 CALCULATING THE SCATTERING AMPLITUDE IN A FINITE VOLUME	19
4 ANALYSIS	21
4.1 Kaon - Nucleon Scattering in Chiral Perturbation Theory	21
4.2 Extrapolating to the Physical value of $\mu_{kn}a_{kn}$	23

5 CONCLUSION 24
LIST OF REFERENCES 26

LIST OF TABLES

2.1	The parameters of the MILC gauge configurations and domain-wall propagators that were used in this work. The subscript l denotes light quark (up/down) where s denotes the strange quark. The superscript dwf denotes the bare quark mass for the domain wall fermion propagator calculation. The last column is the number of configurations times the number of sources for each configuration. Each of this dataset refers to the Ensemble 2064f21b681.	15
2.2	The following results are from the lattice calculations. The statistical errors were computed using the jackknife method of error estimation. The systematic errors were computed by shifting the fitting range and recalculating the parameters, then subtracting the results and dividing by 2. The quantity in the square brackets is the fitting range for each particular mass. The errors listed for the product of the reduced mass and the scattering length are the statistical first and the systematic second.	16
4.1	The following table contains the results from the two different polynomial fits that were employed to calculate C_1	23
4.2	This table is comprised of values of $\mu_{kn}a_{kn}$ that were calculated by inserting the physical values of μ_{kn}, F_k , and M_k into eq. 47 and then using the 4 different values for C_1 that were obtained in the last part.	23

LIST OF FIGURES

1-1	Here we see the constituent quark content of the neutron.	3
1-2	As we apply energy to the neutron at first the quarks begin to move apart.	3
1-3	As we continue to apply energy to the neutron we find that instead of freeing the quarks we instead create quark, anti-quark pairs. This is due to the fact that the energy required to separate the constituent quarks is roughly 1GeV per fm , which is far above the threshold for pair production.	4
1-4	Here we see three of the infinitely many different paths between the point A at a time t_0 and the point B at time t_f	5
2-1	These plots are of the reduced mass times the effective scattering length as a function of lattice time. The first plot is of the $b * m = 007$ mass, the second plot is the $b * m = 010$ mass, the third plot is of the $b * m = 020$ mass, and the fourth plot is of the $b * m = 030$ mass.	17
5-1	This is a plot of $\mu_{kn} a_{k-n}$ as a function of μ_{kn}/f_k . The red line is the chiral perturbation prediction, while the blue line is the physical prediction. The points are the results for the 007, 010, 020, and 030 masses respectively.	25

ABSTRACT

KAON NUCLEON SCATTERING IN LATTICE QCD

by

ANTHONY CHARLES MARCOLONGO
University of New Hampshire, September, 2007

In this paper I discuss why one would want to study meson baryon interactions within the framework of lattice QCD, and what I have contributed to this area of research. I begin with a little background on QCD, and Chiral theories. I analyze Kaon Nucleon scattering, and calculate the Kaon Nucleon scattering length from data obtained using a lattice QCD simulation. Therefore, I show that it is possible to use Lattice QCD simulation to extract observables. This is important in areas where experiments are challenging or impossible with current technologies.

CHAPTER 1

BACKGROUND

The reason that we chose to study kaon nucleon interactions, is that the kaon is the second lightest meson, meaning that this is still a relatively low energy process and does not contain some of the complications that higher energy processes suffer from. The only lower energy process in the meson - baryon sector is πN scattering, but that process cannot be studied in Lattice QCD due to the fact that it contains disconnected diagrams. Outside of Lattice QCD πN scattering has already been analyzed by many different groups. Ref. [1] and Ref. [2] among others. One of the major difficulties inherent in QCD is that QCD is not explicitly solvable due to the fact that the coupling constant approaches 1 in the low energy regime, making a perturbative expansion in the coupling constant unfeasible. To counteract this we will instead replace the continuous 4-dimensional space-time with a cubic lattice. The reason for doing this is that we can then replace the infinite dimensional integrals that plague QCD with finite sums. Also by putting our system onto a lattice we introduce a new small, dimensionful, parameter into the equations, namely the lattice spacing b . Once we are finished with our calculations we can then extrapolate our results to the physical world by taking $b \rightarrow 0$, and $L \rightarrow \infty$. The spatial volume of our lattice is given by L^3 . We hope that by following this prescription we will arrive at a physically meaningful result, once we reach the end of our journey.

1.1 General QCD

QCD, Quantum ChromoDynamics, is the theory of the strong nuclear force. QCD is a special kind of Quantum Field Theory, one that is derived from a non-abelian gauge theory.

Non-abelian simply means non commutative, i.e. $a \times b \neq b \times a$. When a Lagrangian is invariant under a transformation which is identically performed at each and every space-time point, that Lagrangian is said to possess a global symmetry. Gauge theory further extends this idea by also requiring that the Lagrangian's in question must also possess local symmetries, meaning that it should be possible to perform these symmetry transformations in a particular region of space-time without affecting what happens in another region. QCD, as a fundamental theory of nature, has several properties that set it apart from other such theories.

- The first being asymptotic freedom. In very high energy reactions quarks and gluons interact very weakly. To put this another way, as you decrease the separation between the particles the force of binding between them also decreases. If a theory is asymptotically free, or not, can be determined by calculating the beta-function for the theory in question. The beta-function describes the variation of the theory's coupling constant under the action of the renormalization group. Ref. [3] For sufficiently short distances, or large energies, an asymptotically free theory can be solved using basic perturbation theory calculations involving Feynman diagrams.

To calculate the beta-function one needs only to evaluate all the Feynman diagrams that contribute to the interactions of the quarks, either by emitting or absorbing a gluon. In non-abelian gauge theories like QCD, the existence of asymptotic freedom depends on the particular gauge group and the number of flavors of interacting particles. To lowest nontrivial order, the beta-function in an $SU(N)$ gauge theory with n_f kinds of different quarks is

$$\beta_1(\alpha) = \frac{\alpha^2}{\pi} \left(-\frac{11N}{6} + \frac{n_f}{3} \right) \quad (1.1)$$

where α is the theory's equivalent of the fine-structure constant from electricity and magnetism, $g^2/(4\pi)$ in natural units. If this function happens to be negative, then the theory is asymptotically free. For $SU(3)$, which is the color charge gauge group

of QCD, the theory is shown to be asymptotically free for $n_f < 16$.

- The next property that sets QCD apart from other theories is that as the separation between quarks is increased the coupling also increases. This property is known as confinement. Ref. [4] This means that the force between quarks does not diminish as the separation between them is increased, unlike Gravity and *E&M*. This implies that it would require an infinite amount of energy to fully separate 2 quarks.

Consider for a moment a nucleon composed of three quarks. As more and more energy is pumped into the system the constituent particles will begin to move further and further apart, but long before they are separated enough to consider them "free" you will have pumped in enough energy to create a new quark anti-quark pair. So instead of winding up with a free quark and a free anti-quark, you get a meson and a baryon and no free quarks. This process is illustrated in figures 1-1, 1-2, and 1-3.

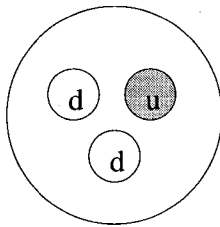


Figure 1-1: Here we see the constituent quark content of the neutron.

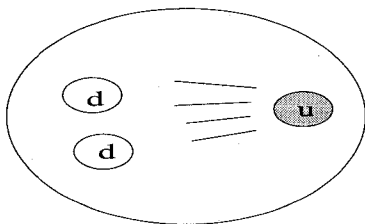


Figure 1-2: As we apply energy to the neutron at first the quarks begin to move apart.

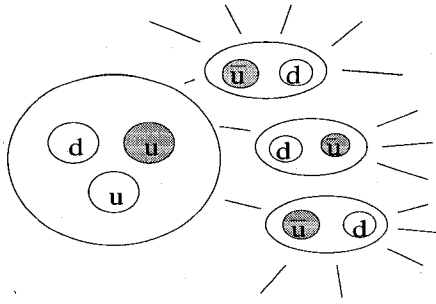


Figure 1-3: As we continue to apply energy to the neutron we find that instead of freeing the quarks we instead create quark, anti-quark pairs. This is due to the fact that the energy required to separate the constituent quarks is roughly 1GeV per fm , which is far above the threshold for pair production.

1.2 Mesons and Baryons

The process that we are interested in studying is one that contains both mesons and baryons. Baryons and mesons both belong to the family of particles known as hadrons, which simply means that they are composed of quarks.

- A meson is a strongly interacting boson. A boson is a particle that contains an integer spin. In the Standard Model of particle physics Ref. [5], the mesons are composite particles composed of an even number of quarks and anti-quarks. All of the known mesons are believed to consist of a quark-antiquark pair, the so-called valence quarks, plus a "sea" of virtual quark-antiquark pairs and virtual gluons. The meson that we are interested in, in this paper, are the kaons. Kaons are the second lightest of the mesons, with the pion being the lightest. All kaons contain either a strange quark or an anti-strange quark, along with either an up/anti-up quark, or a down/anti-down quark.
- The baryons are a family of subatomic particles which are made up of three quarks. The baryons are fermions, which means that they are particles containing half-integer spin. Baryons are strongly interacting that is, they experience the strong nuclear force and are described by Fermi-Dirac statistics, which apply to all particles obeying the Pauli exclusion principle. This is in contrast to the bosons, which do not

obey the Exclusion principle. The baryon that we are interested in is the neutron. Neutrons are made up of 2 down quarks and one up quark.

1.3 The Path Integral Formulation of Quantum Mechanics

The path integral formulation of quantum mechanics Ref. [6] is a description of quantum theory, in which the action principle of classical mechanics is generalized. The idea of the path integral is that we can replace the classical notion of a single, unique history for a system with a sum, or functional integral, over an infinity of possible histories, and then use this new functional integral to compute the quantum amplitude. An illustration of the many paths between two points can be seen in Figure 1-4.

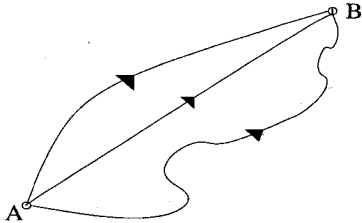


Figure 1-4: Here we see three of the infinitely many different paths between the point A at a time t_0 and the point B at time t_f .

The path integral formulation of quantum mechanics is based on the following postulates of Feynman:

- (a) That the probability for any fundamental event to occur, is given by the square modulus of some complex amplitude.
- (b) That the amplitude for some event to occur is given by summing together all the histories which include that event.
- (c) The amplitude that each history contributes is proportional to $e^{iS/\hbar}$, where S is the action of that particular history.

In order to calculate the overall probability amplitude for a given process, one just needs to add up, the contributions from the different amplitudes contained in postulate 3, over the space of all possible histories of the system in between it's initial and final states, even including histories that are absurd by classical standards. The path integral includes all histories, even ones in which the particle undergoes elaborate and highly unlikely maneuvers. The path integral formulation assigns all of them, no matter how unlikely, amplitudes of equal magnitude. The only difference between the amplitudes are their phases, or the argument of the complex part of the expression. The contributions that differ significantly from the classical history are suppressed by the interference of similar histories caused by the different phases between them. To put this another way, for the paths that lay far from the stationary points of the action, the complex phase of the amplitude, calculated according to postulate 3, will vary rapidly for similar paths, and these amplitudes will tend to cancel each other out.

1.3.1 Slicing the Time Dimension

For a particle located in a smooth potential, the path integral can be approximated as the small-step limit over zig-zag paths, which in one dimension is just the product of ordinary integrals. To describe the motion of a particle from initial position x_0 at time 0 to final position x_n at time t , the time interval can be divided up into n segments, each of fixed duration t . This process is known as time slicing. An approximation for the path integral can be computed as proportional to

$$\int_{-\infty}^{+\infty} \dots \int_{-\infty}^{+\infty} \exp\left(\frac{i}{\hbar} \int H(x_1, \dots, x_{n-1}, t) dt\right) dx_1 \dots dx_{n-1} \quad (1.2)$$

where H is the entire history in which the particle travels from its initial position to its final position between all the possible values of

$$x_j = x(j\Delta t). \quad (1.3)$$

In the limit of $n \rightarrow \infty$, this quantity then becomes a functional integral.

1.3.2 The Path Integral and the Partition Function

The path integral is just the generalization of the integral above to all quantum mechanical problems

$$Z = \int Dx e^{iS[x]/\hbar} \quad (1.4)$$

where

$$S[x] = \int_0^T dt L[x(t)] \quad (1.5)$$

is the action of the classical problem in which one investigates the path starting at time $t = 0$ and ending at time $t = T$, and Dx denotes integration over all paths. In the classical limit, $\hbar \rightarrow 0$, the path of minimum action dominates the integral, because the phase of any path away from this fluctuates rapidly and different contributions cancel.

1.3.3 Wick Rotation

A Wick Rotation Ref. [7] is a method by which one finds a solution to a problem in Minkowski space from a solution to a related problem in Euclidean space, by means of analytic continuation. Ref. [8]

It is motivated by the observation that the Minkowski metric:

$$ds^2 = dx^2 + dy^2 + dz^2 + (-dt^2) \quad (1.6)$$

and the four-dimensional Euclidean metric:

$$ds^2 = dt^2 + dx^2 + dy^2 + dz^2 \quad (1.7)$$

are not distinct quantities if one allows the coordinate t to take on complex values. The

Minkowski metric then becomes Euclidean if t is restricted to values along the imaginary axis. Taking an expression in Minkowski space with coordinates x, y, z, t , and substituting $w = it$, yields a problem in real Euclidean coordinates x, y, z, w which is sometimes easier to solve.

The unitary evolution operator of a particular state, in the Schrodinger picture, is given by:

$$|\alpha; t\rangle = e^{-iHt/\hbar}|\alpha; 0\rangle \quad (1.8)$$

where the state is evolved from some starting time, $t = 0$. If one makes a Wick rotation on this state, and finds the amplitude to go from any state, back to the same state in (imaginary) time iT , it is given by:

$$Z = \text{Tr}[e^{-HT/\hbar}] \quad (1.9)$$

which is precisely the partition function of statistical mechanics for the same system at temperature $1/T\hbar$.

1.4 Lattice QCD

This is a formulation of QCD where the the continuous grid of space time is replaced with a periodic lattice. Ref. [9] Both analytic and perturbative solutions in QCD are either very hard or impossible to come by due to the highly nonlinear nature of the strong force. The formulation of QCD on a discrete lattice rather than a continuous space-time naturally introduces a momentum cut off at the order $1/b$, where b is the lattice spacing, which regularizes the theory. There are several ways to arrive at a cutoff of $1/b$ for the momentum states. The simplest is to use the fact that we are trying to solve a problem involving both relativity and quantum mechanics. For simplicity we work in natural units, $\hbar = c = 1$. In natural units the Heisenberg Uncertainty Principle becomes $\Delta p \Delta x = 1$. Solving for Δp we find that $\Delta p = 1/\Delta x$. The only constant that we have with units of length, that is defined on our lattice, is b . As a result of this cutoff procedure lattice QCD

is mathematically well-defined within our region of interest.

1.4.1 Discretizing the Action

From the work of G. P. Lepage Ref. [9] we know that the continuum action for QCD is:

$$S = \int d^4x \frac{1}{2} \sum_{\mu, \nu} \text{Tr} F_{\mu\nu}^2(x) \quad (1.10)$$

where the function F is given by:

$$F_{\mu\nu} \equiv \partial_\mu A_\nu - \partial_\nu A_\mu + ig[A_\mu, A_\nu] \quad (1.11)$$

The defining characteristic of this particular theory is that it is invariant with respect to all gauge transformations of the following form:

$$F_{\mu\nu} \rightarrow \Omega(x) F_{\mu\nu} \Omega(x)^\dagger \quad (1.12)$$

with $\Omega(x)$ an arbitrary x dependent $SU(3)$ matrix. We now replace the A'_μ s with functions U_μ because it is actually impossible to formulate a lattice version of QCD in terms of the A'_μ s that maintains exact gauge invariance. The U_μ obeys the following transformation properties:

$$U_\mu(x) \rightarrow \Omega(x) U_\mu(x) \Omega(x + a\hat{\mu})^\dagger \quad (1.13)$$

The U'_μ s are $SU(3)$ matrices referred to as linking variables. The Wilson loop function is:

$$W(C) \equiv \frac{1}{2} \text{Tr} P e^{-i \oint_C g A \cdot dx} \quad (1.14)$$

Where C is any closed path built of links on the lattice. Now we want to build a Lagrangian out of the link operators. The Lagrangian that we build must be gauge invariant, local, and symmetric with respect to an exchange of the axis. Starting with the link operators,

the most local non-trivial operator that can be constructed is the "plaquette operator".

$$P_{\mu\nu} \equiv \frac{1}{3} \text{ReTr}(U_\mu(x)U_\nu(x + a\hat{\mu})U_\mu^\dagger(x + a\hat{\mu} + a\hat{\nu})U_\nu^\dagger(x)) \quad (1.15)$$

We then use a standard operator product expansion to find out the traditional "Wilson action" is given by the following expression:

$$S_{Wil} = \beta \sum_{x,\mu>\nu} (1 - P_{\mu\nu}(x)) \quad (1.16)$$

With $\beta = \frac{6}{g^2}$. Expanding S_{Wil} to order a^2 we find:

$$S_{Wil} = \int d^4x \sum_{\mu,\nu} \left(\frac{1}{2} \text{Tr} F_{\mu\nu}^2 + \frac{a^2}{24} \text{Tr} F_{\mu\nu} (D_\mu^2 + D_{\nu\nu}^2) F_{\mu\nu} + \dots \right) \quad (1.17)$$

Next we define the rectangle operator as:

$$R_{\mu\nu} = 1 - \frac{4}{6} a^4 \text{Tr}(gF_{\mu\nu})^2 - \frac{4}{72} a^6 \text{Tr}(gF_{\mu\nu} (4D_\mu^2 + D_\nu^2) gF_{\mu\nu}) - \dots \quad (1.18)$$

We now combine the rectangle operator with the plaquette operator to obtain the improved classical lattice action:

$$S_{classical} = \int d^4x \sum_{\mu,\nu} \frac{1}{2} \text{Tr} F_{\mu\nu}^2 + \vartheta(a^4) \quad (1.19)$$

1.4.2 Chiral Symmetry

In quantum field theory, chiral symmetry Ref. [10] is a possible symmetry of the Lagrangian under which the left-handed and right-handed parts of Dirac fields transform independently. The chiral symmetry transformation can be divided into a component that treats the left-handed and the right-handed parts equally, known as vector symmetry, and a component that actually treats them differently, known as axial symmetry.

Example: u and d quarks in QCD:

Consider quantum Chromodynamics (QCD) with two massless quarks u and d. The

Lagrangian is

$$\mathcal{L} = \bar{u}i\not{D}u + \bar{d}i\not{D}d + \mathcal{L}_{\text{gluons}} \quad (1.20)$$

In terms of left-handed and right-handed spinors it becomes

$$\mathcal{L} = \bar{u}_L i\not{D}u_L + \bar{u}_R i\not{D}u_R + \bar{d}_L i\not{D}d_L + \bar{d}_R i\not{D}d_R + \mathcal{L}_{\text{gluons}} \quad (1.21)$$

Defining

$$q = \begin{bmatrix} u \\ d \end{bmatrix} \quad (1.22)$$

it can be written as

$$\mathcal{L} = \bar{q}_L i\not{D}q_L + \bar{q}_R i\not{D}q_R + \mathcal{L}_{\text{gluons}} \quad (1.23)$$

The Lagrangian is unchanged under a rotation of q_L by any 2×2 unitary matrix L , and q_R by any 2×2 unitary matrix R . This symmetry of the Lagrangian is called flavor symmetry or chiral symmetry, and denoted as $U(2)_L \times U(2)_R$. It can be decomposed into

$$SU(2)_L \times SU(2)_R \times U(1)_V \times U(1)_A \quad (1.24)$$

The vector symmetry $U(1)_V$, acts as

$$q_L \rightarrow e^{i\theta} q_L \quad q_R \rightarrow e^{i\theta} q_R \quad (1.25)$$

and corresponds to baryon number conservation.

The axial symmetry $U(1)_A$, acts as

$$q_L \rightarrow e^{i\theta} q_L \quad q_R \rightarrow e^{-i\theta} q_R \quad (1.26)$$

and it does not correspond to a conserved quantity because it is violated due to quantum anomaly.

The remaining chiral symmetry $SU(2)_L \times SU(2)_R$ turns out to be spontaneously broken by the quark condensate into the vector subgroup $SU(2)_V$, known as isospin. The Goldstone bosons Ref. [11] corresponding to the three broken generators are the pions, π^- , π^0 , and π^+ . In the real world, because of the masses of the quarks and electromagnetism, $SU(2)_L \times SU(2)_R$ is only an approximate symmetry to begin with, therefore the pions are not massless, but have small masses: they are pseudo-Goldstone bosons.

1.4.3 Chiral Perturbation Theory

This an effective field theory constructed on a Lagrangian consistent with the (approximate) chiral symmetry of quantum ChromoDynamics, as well as the other symmetries of parity and charge conjugation. Ref. [12] The Lagrangian is constructed by introducing every possible interaction of particles which is not expressly excluded by symmetry, and then ordering them based on the number of momentum and mass powers (so that $(\partial\pi)^2 + m_\pi\pi^2$ is considered in the first approximation, and terms like $m_\pi^4\pi^2 + (\partial\pi)^6$ are used as higher order corrections). It is also common to compress the Lagrangian by replacing the single pion fields in each term with an infinite series of all possible combinations of pion fields. One of the most common choices is

$$U = \exp\left(\frac{i}{f_\pi} \begin{pmatrix} \pi^0 & \sqrt{2}\pi^+ \\ \sqrt{2}\pi^- & -\pi^0 \end{pmatrix}\right) \quad (1.27)$$

This theory allows for the description of interactions between pions, and between pions and nucleons (or other matter fields). $SU(3)$ ChPT can also describe interactions of kaons and eta mesons, while similar theories can be used to describe the vector mesons. We use $SU(3)$ to describe these processes because we are only interested in quarks up to and including the strange, so we can ignore the heavy flavors of quark (charm, bottom and top). Since chiral perturbation theory assumes chiral symmetry, and therefore massless quarks, it cannot be used to model interactions of the heavier quarks.

In some cases, chiral perturbation theory has been successful in describing the inter-

actions between hadrons in the non-perturbative regime of the strong interaction. For instance, it can be applied to few-nucleon systems, and at next-to-next-to-leading order in the perturbative expansion, it can account for three-nucleon forces in a natural way.

CHAPTER 2

DETAILS OF THE LATTICE CALCULATION

2.1 Details of the Lattice Calculation

This computation used the mixed-action lattice QCD scheme developed by LHPC [13, 14] in which domain-wall valence quarks from a smeared-source are placed on $N_f = 2 + 1$ asqtad-improved [15, 16] MILC configurations generated with rooted staggered sea quarks that are hyper-cubic-smeared. The strange-quark mass, which was used to generate the MILC configurations, was fixed near its physical value, $bm_s = 0.050$. This value was determined by the mass of hadrons containing strange quarks. Using Dirichlet boundary conditions we are able to reduce the original time dimension of 64 slices down to only 32 slices. This choice of boundary conditions allowed us to reuse the propagators that were already computed for the nucleon structure function calculations performed by LHPC. The quantity that I set out to calculate is the scattering length, to do that we first need to calculate the difference in energy between the interacting and the non-interacting particles. To this end we first calculated the one-kaon correlation function $C_{K^-}(t)$, the one-nucleon correlation function $C_N(t)$, and the kaon-nucleon correlation function $C_{K^-N}(p,t)$, where t denotes the number of time slices between the sink and the source, and p is the magnitude of the momentum of each particle. Values for quark masses for the different ensembles are

Table 2.1: The parameters of the MILC gauge configurations and domain-wall propagators that were used in this work. The subscript l denotes light quark (up/down) where s denotes the strange quark. The superscript dwf denotes the bare quark mass for the domain wall fermion propagator calculation. The last column is the number of configurations times the number of sources for each configuration. Each of this dataset refers to the Ensemble 2064f21b681.

Ensemble	bm_l	bm_s	bm_l^{dwf}	bm_s^{dwf}	$10^3 \times bm_{res}$	# of propagators
m007m050	0.007	0.050	0.0081	0.081	1.604 ± 0.038	468×4
m010m050	0.010	0.050	0.0138	0.081	1.552 ± 0.027	658×4
m020m050	0.020	0.050	0.0313	0.081	1.239 ± 0.028	486×3
m030m050	0.030	0.050	0.0478	0.081	0.982 ± 0.030	564×6

listed in Table 2.1. The single-kaon correlation function is Ref. [17]

$$C_{K^-}(t) = \sum_{\mathbf{x}} \langle K^+(t, \mathbf{x}) K^-(0, \mathbf{0}) \rangle , \quad (2.1)$$

where the summation over \mathbf{x} corresponds to summing over all the spatial lattice sites, thereby projecting onto the momentum $\mathbf{p} = \mathbf{0}$ state. The single-nucleon correlation function has a similar form. The K^-N correlation function that projects onto the s-wave state in the continuum limit is

$$C_{K^-N}(p, t) = \sum_{|\mathbf{p}|=p} \sum_{\mathbf{x}, \mathbf{y}} e^{i\mathbf{p} \cdot (\mathbf{x} - \mathbf{y})} \langle K^+(t, \mathbf{x}) N(t, \mathbf{y}) N(0, \mathbf{0}) K^-(0, \mathbf{0}) \rangle , \quad (2.2)$$

where, in eqs. (15) and (16), $K^-(t, \mathbf{x}) = u(t, \mathbf{x}) \gamma_5 \bar{s}(t, \mathbf{x})$ is an interpolating field for the K^- , and $N(t, \mathbf{x}) = \epsilon^{abc} [d^{Ta}(t, \mathbf{x}) C \gamma_5 u^b(t, \mathbf{x})] d^c(t, \mathbf{x})$ is an interpolating field for the N . Where $C = \gamma_4 \gamma_2$, a, b, c , are the color indices, and T denotes taking the transpose. In the relatively large lattice volumes that we are using, the energy difference between the interacting and non-interacting two-particle states is a small fraction of the total energy, which is dominated by the masses of the particles. In order to extract this energy difference we formed the ratio of correlation functions, $G_{K^-N}(p, t)$, where

$$G_{K^-N}(p, t) \equiv \frac{C_{K^-N}(p, t)}{C_{K^-}(t) C_N(t)} \rightarrow \sum_{n=0}^{\infty} \mathcal{A}_n e^{-\Delta E_n t} , \quad (2.3)$$

and the arrow becomes an equality in the limit of an infinite number of gauge configurations. In $G_{K-N}(p, t)$, some of the fluctuations that contribute to both the one- and two-particle correlation functions cancel, thereby improving the quality of the extraction of the energy difference beyond what we are able to achieve from an analysis of the individual correlation functions.

To extract the energy splitting it is necessary to form the ratio of the correlation functions at two consecutive times, and then take the Log of that ratio.

$$\Delta E_{K-N}(t) = \log \left(\frac{G_{K-N}(0, t)}{G_{K-N}(0, t+1)} \right), \quad (2.4)$$

Table 2.2: The following results are from the lattice calculations. The statistical errors were computed using the jackknife method of error estimation. The systematic errors were computed by shifting the fitting range and recalculating the parameters, then subtracting the results and dividing by 2. The quantity in the square brackets is the fitting range for each particular mass. The errors listed for the product of the reduced mass and the scattering length are the statistical first and the systematic second.

Ensemble	m_K/f_K	m_N/f_K	μ_{KN}/f_K	δE_{KN} (MeV)	$\mu_{KN} a_{K-N}$
m007[8-10]	3.39765 ± 0.06138	6.3382 ± 0.88882	2.21193 ± 0.94165	14.6845 ± 1.75162	$-0.501642 \pm 0.84854 \pm 0.07143$
m010[7-9]	3.5072 ± 0.086982	6.91351 ± 0.56922	2.32681 ± 0.81820	20.9068 ± 1.48488	$-0.704285 \pm 0.67672 \pm 0.02651$
m020[7-9]	3.71547 ± 0.09904	7.47454 ± 0.506024	2.4818 ± 0.7351	9.8946 ± 1.06578	$-0.457762 \pm 0.28406 \pm 0.01116$
m030[9-11]	3.83415 ± 0.0675	7.83961 ± 0.34476	2.57485 ± 0.51637	10.0749 ± 0.53244	$-0.516196 \pm 0.05527 \pm 0.00572$

This ratio in the limit of infinite gauge configurations and at large times becomes a constant that is equal to the lowest energy of the interacting kaon and nucleon in the volume. At each time-slice, $\Delta E_{K-N}(t)$ is inserted into eqs.(3.3) and (3.1), or into eq. (3.4), to give a scattering length at each time slice, $a_{K+N}(t)$. It is actually more useful to consider the dimensionless quantity of the reduced mass times the scattering length, $\mu_{KN} a_{K-N}$, in our analysis, where $\mu_{KN}(t)$, the “effective reduced mass” is constructed from the effective mass of the single particle correlators. Table 2.2 is a collection of the different quantities that were calculated on the lattice for each of the ensembles.

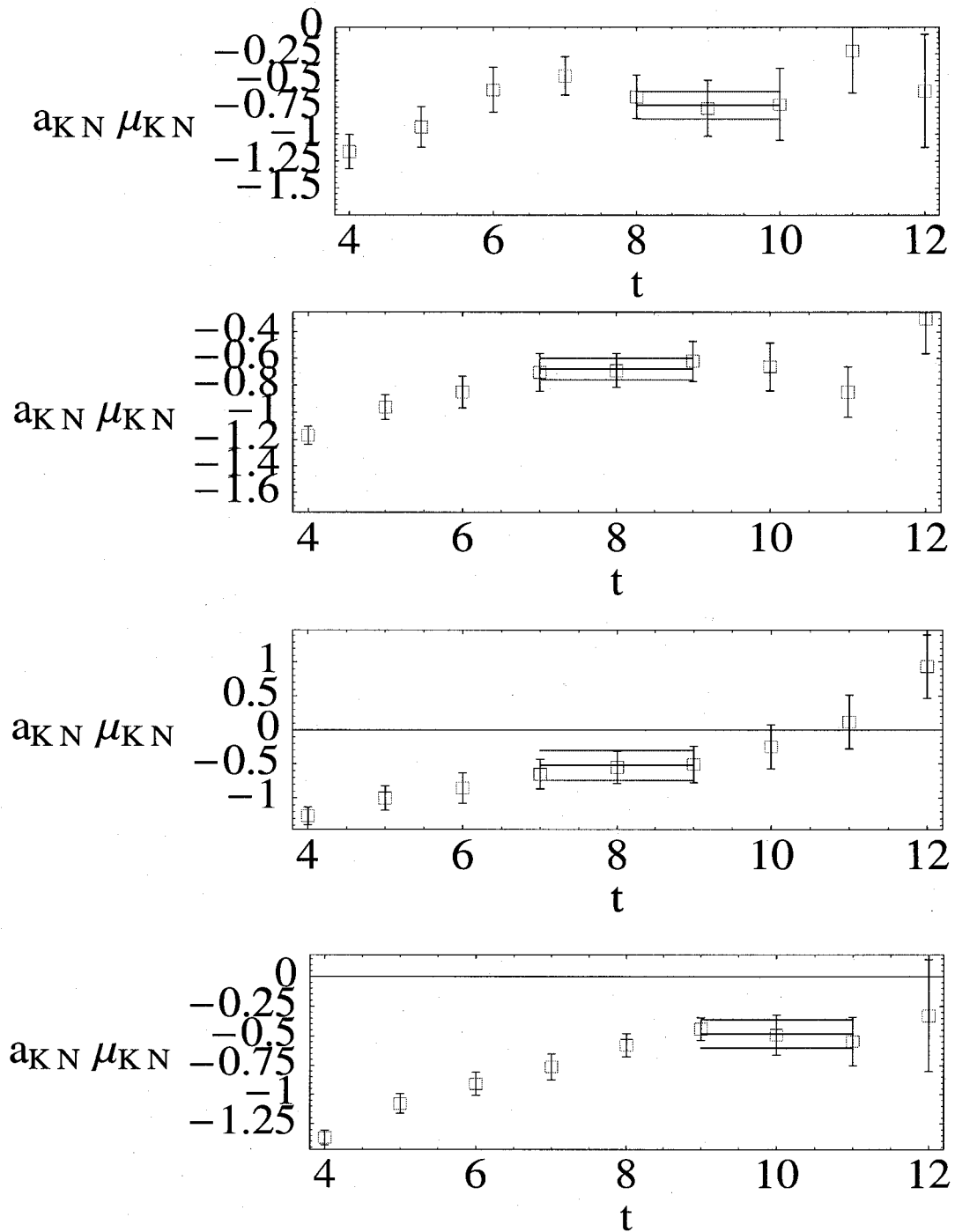


Figure 2-1: These plots are of the reduced mass times the effective scattering length as a function of lattice time. The first plot is of the $b * m = 007$ mass, the second plot is the $b * m = 010$ mass, the third plot is of the $b * m = 020$ mass, and the fourth plot is of the $b * m = 030$ mass.

For each of the MILC ensembles that we analyze, the effective scattering lengths are shown in fig. 2-1

CHAPTER 3

CALCULATING THE SCATTERING AMPLITUDE IN A FINITE VOLUME

In order to calculate the s-wave scattering amplitude for 2 particles that are below the inelastic threshold we will use Lüscher's method [18]. We know that for two particles that have masses m_1 and m_2 and are in an s-wave, possessing zero total three momentum, and located in a finite volume, the difference between the energy levels of the particles and the energy levels of two non-interacting particles can be related to the inverse scattering amplitude via the eigenvalue equation

$$p \cot \delta(p) = \frac{1}{\pi L} \mathbf{S} \left(\frac{pL}{2\pi} \right) , \quad (3.1)$$

where $\delta(p)$ is the elastic-scattering phase shift, and the regulated three-dimensional sum is

$$\mathbf{S}(\eta) \equiv \sum_{\mathbf{j}}^{\|\mathbf{j}\| < \Lambda} \frac{1}{\|\mathbf{j}\|^2 - \eta^2} - 4\pi\Lambda . \quad (3.2)$$

The sum in eq. (3.2) is over all integers \mathbf{j} such that $\|\mathbf{j}\| < \Lambda$ and the limit $\Lambda \rightarrow \infty$ is implicit. This definition is the same as the analytic continuation of zeta-functions which was presented by Lüscher. In eq. (3.1), L is the length of the spatial dimension in a cubically-symmetric lattice. The energy eigenvalue E_n and its deviation from the sum of the rest masses of the particle, ΔE_n , are related to the center-of-mass momentum p_n , a

solution of eq. (3.1), by

$$\begin{aligned}\Delta E_n &\equiv E_n - m_1 - m_2 = \sqrt{p_n^2 + m_1^2} + \sqrt{p_n^2 + m_2^2} - m_1 - m_2 \\ &= \frac{p_n^2}{2\mu_{12}} + \dots ,\end{aligned}\tag{3.3}$$

where μ_{12} is the reduced mass of the system. In the case in which there are no interactions between the particles, $|p \cot \delta| = \infty$, and the corresponding energy levels occur at momenta $\mathbf{p} = 2\pi\mathbf{j}/L$, which are just the single-particle modes in a cubic cavity. Expanding eq. (3.1) about zero momenta, $p \sim 0$, one obtains the familiar relation:

$$\Delta E_0 = -\frac{2\pi a}{\mu_{12}L^3} \left[1 + c_1 \frac{a}{L} + c_2 \left(\frac{a}{L} \right)^2 \right] + \mathcal{O} \left(\frac{1}{L^6} \right) ,\tag{3.4}$$

with

$$\begin{aligned}c_1 &= \frac{1}{\pi} \sum_{\substack{|\mathbf{j}| < \Lambda \\ \mathbf{j} \neq \mathbf{0}}} \frac{1}{|\mathbf{j}|^2} - 4\Lambda = -2.837297 , \\ c_2 &= c_1^2 - \frac{1}{\pi^2} \sum_{\substack{|\mathbf{j}| < \Lambda \\ \mathbf{j} \neq \mathbf{0}}} \frac{1}{|\mathbf{j}|^4} = 6.375183 ,\end{aligned}\tag{3.5}$$

and a is the scattering length, defined by

$$a = \lim_{p \rightarrow 0} \frac{\tan \delta(p)}{p} .\tag{3.6}$$

CHAPTER 4

ANALYSIS

4.1 Kaon - Nucleon Scattering in Chiral Perturbation Theory

What we would like to do is to get a prediction for the kaon nucleon scattering length from χpt at tree level. Ref. [19] We begin with the general form of the T matrix elements for meson baryon scattering at tree level:

$$T_{mb} = 4\pi a_{mb} \left(1 + \frac{M_m}{M_b} \right) \quad (4.1)$$

With

$$T_{kn} = -\frac{M_k}{F_k^2}, \quad F_k = 113 MeV \quad (4.2)$$

We then plug eq. (4.2) into eq. (4.1) and solve for a_{kn} . We find that:

$$a_{kn} = -\frac{M_k}{4\pi F_k^2} \frac{M_n}{M_k + M_n} \quad (4.3)$$

This can be simplified to:

$$a_{kn} = -\frac{\mu_{kn}}{4\pi F_k^2} \quad (4.4)$$

Since it is more convenient to work with dimensionless quantities we chose to multiply both side of our scattering length equation by μ_{kn} to arrive at our final expression:

$$\mu_{kn}a_{kn} = -\frac{1}{4\pi} \left(\frac{\mu_{kn}}{F_k} \right)^2 \quad (4.5)$$

Defining x as,

$$x = \frac{\mu_{kn}}{F_k} \quad (4.6)$$

We see that the χ_{pt} prediction at tree level takes the following form:

$$\mu_{kn}a_{kn} = -\frac{1}{4\pi}x^2 \quad (4.7)$$

Next we want to extend this to one loop order.

$$T_{kn}^{NLO} = \left(\frac{M_k}{F_k} \right)^2 C_1 \quad (4.8)$$

Where C_1 has $Dim[E^{-1}]$. Substituting eq. (4.8) back into eq. (4.1) we find an expression for the scattering length at one loop order.

$$a_{kn}^{NLO} = \frac{M_k \mu_{kn}}{4\pi F_k^2} C_1 \quad (4.9)$$

For the purposes of this paper we will let $a^{total} = a^{LO} + a^{NLO}$, and then substitute this into eq. (4.5) we find that:

$$\mu_{kn}a_{kn}^{total} = -\left(\frac{x}{4\pi} \right)^2 (1 - M_k C_1) \quad (4.10)$$

We then found a value for C_1 by taking the scattering length data and then fitting it with a second order polynomial. The values for this fitting procedure are contained in Table 4.1. This allowed us to use a non-linear regression fit to extract the value for C_1 . We did both a weighted fit and a non-weighted fit. For the weights that were used the statistical error and the systematic error was added in quadrature.

Table 4.1: The following table contains the results from the two different polynomial fits that were employed to calculate C_1 .

Fitting Procedure	C1 Value
Polynomial Fit	-0.01632 ± 0.00324
Polynomial Fit with weights	0.03313 ± 0.01553

4.2 Extrapolating to the Physical value of $\mu_{kn}a_{kn}$

Table 4.2: This table is comprised of values of $\mu_{kn}a_{kn}$ that were calculated by inserting the physical values of μ_{kn} , F_k , and M_k into eq. 47 and then using the 4 different values for C_1 that were obtained in the last part.

Fitting Procedure	C1 Value
$\mu_{kn}a_{kn}^{+weighted}$	-0.251406
$\mu_{kn}a_{kn}^{-weighted}$	-0.649586
$\mu_{kn}a_{kn}^{+non-weighted}$	-0.407704
$\mu_{kn}a_{kn}^{-non-weighted}$	-0.490739
$\mu_{kn}a_{kn}^{physical}$	-0.508 ± 0.033

We see that the central value of $\mu_{kn}a_{kn}$ from the 4 different determinations that all but one lay well within the error of $\mu_{kn}a_{kn}^{physical}$ (Determined using the values from Ref. [20]). All values were calculated with a 68 percent confidence level. Table 4.2 contains a summary of the values obtained.

CHAPTER 5

CONCLUSION

In this paper I have shown that it is indeed possible to get physically meaningful results for the K^-N scattering length in fully dynamical QCD at pion masses from $m_\pi \sim 290$ MeV and $m_\pi \sim 600$ MeV. We used the continuum expressions for the scattering lengths in $SU(3)$ chiral perturbation theory in conjunction with the quantities f_K , m_K , and m_N to predict the physical K^-N scattering lengths. For the physical value of a_{k-n} we use $(-0.31 \pm 0.02)fm$ (Ref. [20]). We then multiply that by the physical value of the reduced mass, $\mu_{phys} = 323.6MeV$. We find that $a_{k-n}\mu_{phys} = -0.508 \pm 0.033$, this compares very favorably with the results obtained from the lattice calculation.

After looking at fig. 5-1 it is a simple matter to imagine that as we extrapolate down to the physical quark masses, the lattice predictions will intersect the physical line along the chiral perturbation curve. The next step would be to do a similar analysis for a heavier process, like $\pi\Sigma$.

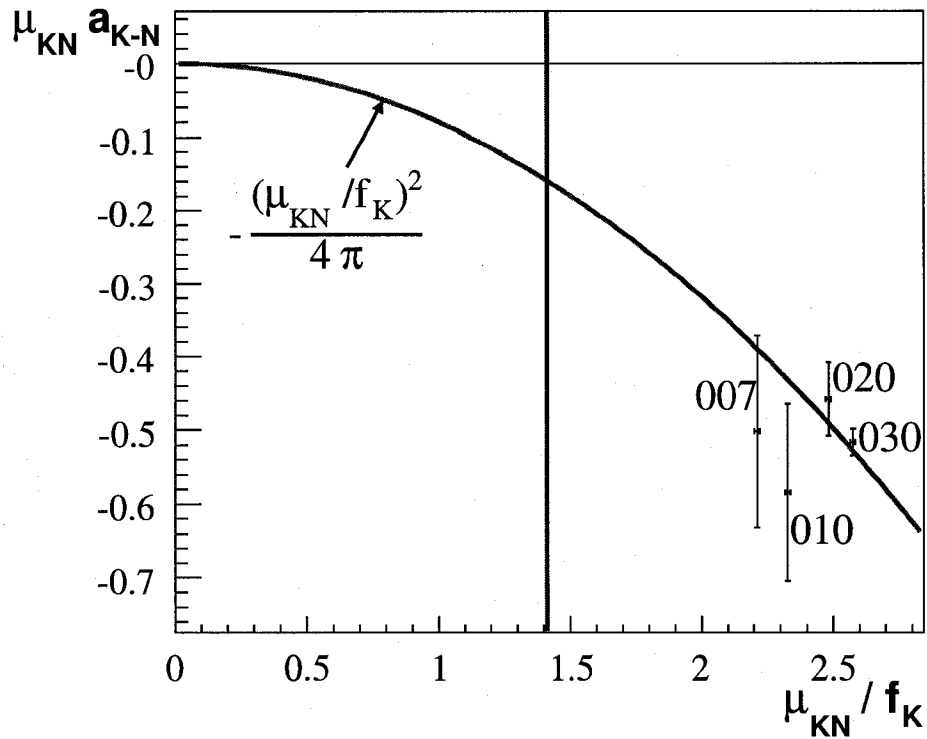


Figure 5-1: This is a plot of $\mu_{kn} a_{k-n}$ as a function of μ_{kn} / f_k . The red line is the chiral perturbation prediction, while the blue line is the physical prediction. The points are the results for the 007, 010, 020, and 030 masses respectively.

LIST OF REFERENCES

- [1] L. Ai W. R. Gibbs and W. B. Kaufmann. Low-energy pion nucleon scattering. *PiN Newslett.*, 1997.
- [2] N. Fettes and U. G. Meissner. Complete analysis of pion nucleon scattering in chiral perturbation theory to third order. *hep-ph/0101030*, 2001.
- [3] K. G. Wilson. The renormalization group and critical phenomena. *Rev. Mod. Phys.*, 1983.
- [4] Z. K. Zhu. *Study Of QCD Confinement*. PhD thesis, DREXEL UNIVERSITY, 1995.
- [5] S. F. Novaes. Standard model: An introduction. *hep-ph/0001283*, 2000.
- [6] C. Morningstar. The monte carlo method in quantum field theory. *hep-lat/0702020*, 2007.
- [7] A. Bogojevic and O. Miskovic. Wick rotation and abelian bosonization. *hep-th/9811074*, 1998.
- [8] S. Ciulli. Stable analytic continuation and unitarity. *Nuovo Cim. A*, 1974.
- [9] G. P. Lepage. Lattice qcd for novices. *hep-lat/0506036*, 1998.
- [10] Z. Liu. *Hadron Properties From Lattice QCD Simulations With Exact Chiral Symmetry*. PhD thesis, Colorado U., 2006.
- [11] M. F. M. Lutz. The relativistic nuclear dynamics for the su(3) goldstone bosons of chiral qcd. *nucl-th/0212021*, 2002.
- [12] B. Borasoy. Introduction to chiral perturbation theory. *hep-ph/0703297*, 2007.
- [13] D. B. Renner *et al.* [LHP Collaboration]. Hadronic physics with domain-wall valence and improved staggered sea quarks. *hep-lat/0409130*, 2004.
- [14] R. G. Edwards *et al.* [LHPC Collaboration]. Hadron structure with light dynamical quarks. *hep-lat/0509185*, 2005.
- [15] D. Toussaint K. Orginos and R. L. Sugar [MILC Collaboration]. Variants of fattening and flavor symmetry restoration. *hep-lat/9903032*, 1999.
- [16] K. Orginos and D. Toussaint [MILC collaboration]. Testing improved actions for dynamical kogut-susskind quarks. *hep-lat/9805009*, 1998.
- [17] S. R. Beane *et al.* pi k scattering in full qcd with domain-wall valence quarks. *hep-lat/0607036*, 2006.
- [18] M. Lüscher. Two particle states on a torus and their relation to the scattering matrix. *hep-lat/0509135*, 1986.

- [19] M. J. Savage. Lambda (1405) contribution to kaon - nucleon scattering lengths in chiral perturbation theory. *hep-ph/9404285*, 1994.
- [20] A. D. Martin. Kaon-nucleon parameters. *Nucl. Phys. B*, 1981.